GEOMETRY INFLUENCE ON THE HALL EFFECT DEVICES PERFORMANCE

Maria-Alexandra PAUN[1], Jean-Michel SALLÈSE[2], Maher KAYAL[3]

The influence of the geometry, via the ratio L/W of the Hall cells and the geometrical correction factor G on several figures of merit regarding Hall sensors is analyzed, namely the sensitivity, Hall Voltage and power dissipated within the device. Experimental values for the parameters of interest are given for eight different geometries integrated in CMOS technology using certain biasing currents. We discuss how these results compare with an analytical model and we propose a global optimization analysis for guiding the designer in best Hall cell dimensions selection.

Keywords: Hall effect sensors, geometrical correction factor, sensitivity, Hall voltage, power dissipated

1. Introduction. Generalities about the Hall effect sensors

Since more than hundred years, Hall effect devices have been used to demonstrate the basic laws of physics, to study details of carrier transport phenomena in solids, to detect the presence of a magnet and as sensing devices for magnetic fields. Generally, the Hall effect takes place in any solid-state electron device exposed to a magnetic field. When a bias current is supplied between two contacts of a Hall plate and a perpendicular magnetic field is applied to the device, a voltage appears between the sense contacts. This voltage is called Hall voltage [1].

Microscopic models have recently been developed to simulate self-consistent electric potentials in Hall devices. Molecular dynamics for the motion of electrons and electron-electron interactions and conformal mapping were used to obtain the Hall potentials, by a computational feasibility method [2].

The Hall voltage is proportional to the vector cross product of the current (I) and the magnetic field (B). It is on the order of few tens of mV in silicon and thus requires amplification for practical applications. Silicon exhibits the

[1] PhD Student, STI-IEL-Electronics Lab (LEG), Ecole Polytechnique Fédérale de Lausanne (EPFL),CH-1015 Lausanne, Switzerland, Corresponding author: maria-alexandra.paun@epfl.ch
[2] Prof., STI-IEL-Electronics Lab (LEG), Ecole Polytechnique Fédérale de Lausanne (EPFL), CH-1015 Lausanne, Switzerland
[3] Prof., STI-IEL-Electronics Lab (LEG), Ecole Polytechnique Fédérale de Lausanne (EPFL), CH-1015 Lausanne, Switzerland

piezoresistance effect, a change in electrical resistance proportional to strain. This effect can be minimized by properly orienting the Hall element on the IC and by using multiple Hall elements. Fig. 1 shows two Hall elements located in close proximity on an IC. They are positioned in such a way that they experience the same packaging stress, represented by ΔR. The first Hall element has its excitation applied along the vertical axis and the second along the horizontal axis. Summing the two outputs eliminates the signal due to stress. Micro switch Hall ICs use two or four elements [3].

2. Basic Hall effect sensors

The Hall element is the basic magnetic field sensor. It requires an amplifier stage and temperature compensation circuitry in order to use it in most applications. Voltage regulation is needed when operating from an unregulated supply. Figure 2 illustrates a basic Hall sensor from the Honeywell reference on Hall sensors. If the Hall voltage is measured when no magnetic field is present, the output should be zero. However this is never satisfied in practice and there is always an offset voltage that should be minimized. According to Popovic's monography, major causes of offset are imperfections in the device fabrication process, such as misalignment of contacts, non-uniformity in material resistivity and thickness. A mechanical stress in combination with the piezoresistance effect can also generate offset.

$$V_{total} = V_{offset} + V_H(B) \tag{1}$$

On the other hand, the potential of each output terminal measured with respect to ground will not be zero. This is the common mode voltage (CMV) that should be equal for both output nodes, therefore the potential difference should ideally be zero. Figure 2 shows a schematic where only the potential difference, the Hall voltage, is amplified, thus rejecting the common mode voltage. The Hall voltage is of the order of 30 mV in the presence of a one gauss magnetic field. This low-level output requires an amplifier with low noise, high input impedance and moderate gain. A differential amplifier with these characteristics can be readily integrated with the Hall element using different technologies on Si, in general CMOS technology. Temperature compensation is also easily integrated.

Since the Hall voltage is a function of the input current, there is a need for a regulator that will maintain a constant current.

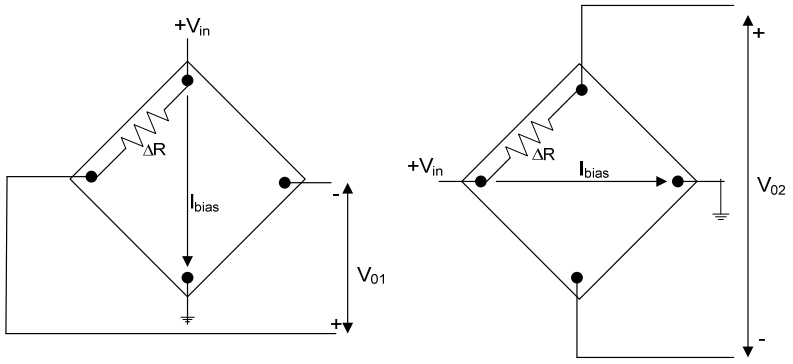

Fig. 1 Hall element orientation

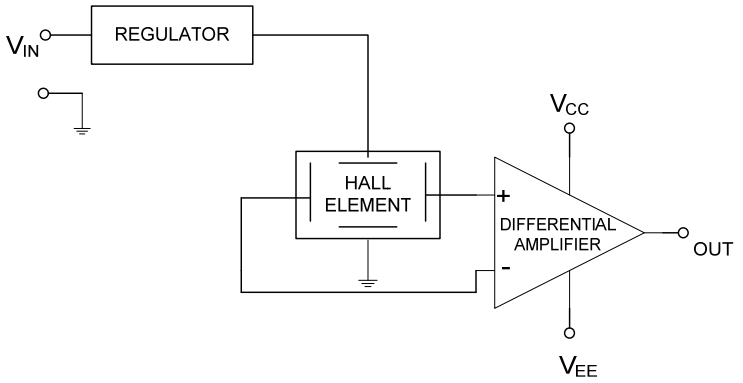

Fig. 2 Basic Hall effect sensor

Today, due to economical considerations, a new class of Hall microsensors with minimal design complexity was developed [4].

3. Classical approach for Hall cells

In the classical approach, the Hall cell is shaped as a Greek cross. The structure has some symmetry and it is invariant by a rotation of $\pi/2$. This allows current-spinning technique to be used for minimizing residual offsets.

The offset depends on many parameters such as technology, temperature and stress. Practically, it limits the minimum magnetic field that can be measured. A classical way of reducing offset is to couple two or four identical cells that are rotated [5]. Hall circuits fabricated in CMOS technology rely on the so-called spinning current method (periodic supply and output-contacts permutations) to enhance the sensor sensitivity [6].

The 3D cross presented in Fig. 3 has 4 contacts (in darker grey shades), among which two used to impose a current (namely *A* and *C*) and others are used

(*B* and *D*) for sensing the Hall voltage. Length and width of the cross are respectively denoted by *L* and *W*, sensing contacts extension is further on denoted by *s*, and the thickness of the active region is referred as *t*.

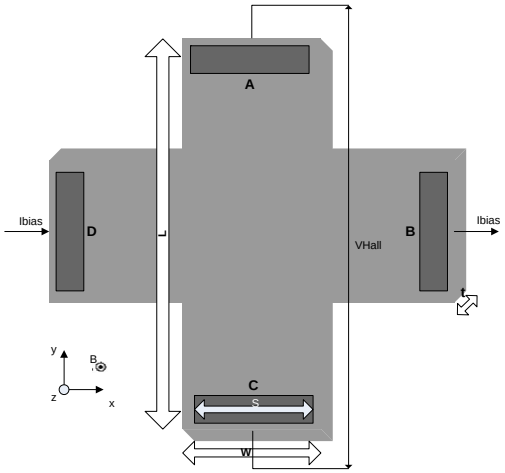

Fig. 3 Classical Greek Cross

To summarize, different quantities are used to characterize the Hall device [1].

The Hall Voltage

The Hall voltage follows the well known relation.

$$V_H(B) = \frac{Gr_H}{nqt} I_{bias} B_\perp \tag{2}$$

where B is the magnetic field component perpendicular to the plane, G is the geometrical correction factor, I_{bias} the biasing current, r_H is the scattering factor of silicon that can be approximated to 1.15, n is the carrier density, q is the magnitude of the electron charge, t is the thickness of the plate and S_I is the current-related sensitivity.

Equivalently, we have

$$V_H(B) = \mu_H \frac{W}{L} GVB_\perp \tag{3}$$

where μ_H is the Hall mobility.

The geometrical correction factor, *G*

In general, the geometrical correction factor G for a Hall device is given by the following relationship

$$G = 1 - \frac{16}{\pi^2} e^{-\frac{\pi L}{2W}} \left(1 - \frac{8}{9} e^{-\frac{\pi L}{2W}}\right)\left(1 - \frac{\theta_H^2}{3}\right) \tag{4}$$

This relation is valid for $0.85 \leq L/W \leq \infty$ and $0 \leq \theta_H \leq 0.45$ radians.

The absolute sensitivity, *S*

The absolute sensitivity of Hall effect sensors is given by:

$$S = \frac{V_H}{B_\perp} = \frac{Gr_H}{nqt} I_{bias} = GS_I I_{bias} \tag{5}$$

where S_I is the current-related sensitivity.
Further on, we have the relationships:

$$S = GS_I I_{bias} \ ; \ S_I = S_{I\max} = \frac{r_H}{nqt} \tag{6}$$

where the geometrical factor G models the reduction of V_{HALL} due to the part of the current which is perturbed from the sensing contacts as well as the short circuit effect induced by the biasing contacts [7].

The power dissipated, *P*

The Hall voltage expressed as function of the dissipated power is

$$V_H(B) = G\left(\frac{W}{L}\right)^{1/2} r_H \left(\frac{\mu}{nqt}\right)^{1/2} (P)^{1/2} B_\perp \tag{7}$$

For certain values of the width-to-length ratio, the dissipated power inside the device can be introduced as:

$$P = \frac{V_H^2}{G^2\left(\frac{W}{L}\right) r_H^2 \left(\frac{\mu}{nqt}\right) B_\perp^2} \tag{8}$$

4. Hall device configurations

Up to 8 geometries implemented in 0.35 μm CMOS technology have been measured and analyzed in terms of specific parameters, such as absolute sensitivity, Hall voltage and power dissipated. All structures are symmetric and invariant to a rotation with π/2. The classical Greek cross was implemented as the basic cell. Further on, the variation of the cell dimensions led us to proposing the cells called L, XL. To avoid piezoresistive effects, the axes of the cells were oriented 45 degrees with respect to the Si crystallographic directions. Leaving the cross behind, we also implemented new shapes, such as as borderless and square structures. The borderless cell has the sensing contacts located inside of the active N-well region in order to minimize as much as possible errors related to the border. A low doped Hall cell with higher absolute sensitivity was also integrated

The resistances of the Hall cells, the dimensions of the active N-well, as well as values for the sensing contacts have been reported in table 1. The narrow contacts,

borderless and square cells have small sensing contacts in comparison with the others in order to satisfy that the condition s/W < 0.18 is fulfilled. The geometrical correction factor has been computed for each individual geometry. For the first five geometries, Eq. (4) was used. For the last three structures, because of the small sensing contacts area, an approximate expression given by Eq. (11) could also be used.

The Hall cells were integrated together with the specific electronics and an automated measurement system was used to measure the specific parameters of the proposed geometries.

5. Results and discussion

An analysis at the device level was performed. The following table summarizes the eight tested geometries and their specific parameters, such as resistance, dimensions of the active area, geometrical correction factor (G), length-to-width ratio *L/W*, etc.

Table 1

Properties of the eight analyzed Hall cells geometries

Geometry Type	***Basic***	***Low-doped***	***L***	***XL***	***45 Deg***	***Narrow Contacts***	***Borderless***	***Square***
Shape	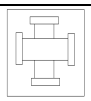	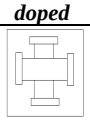	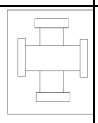	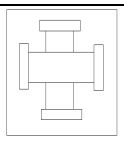		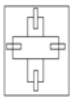	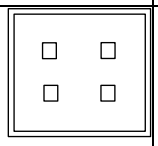	
R_0 (kΩ) at T=300K and B=0T	2.3	5.6	2.2	2.2	2.1	2.5	1.3	4.9
***W, L* (µm) of the Active Area N-well**	W=11.8	W=11.8	W=17.8	W=22.6	W=11.8	W=9.5	W=49.9	W=20
	L=21.6	L=21.6	L=32.4	L=43.2	L=21.64	L=21.6	L=49.9	L=20
***s* (µm) for Sensing Contacts**	S=11	S=11	S=16	S=20.7	S=11	S=1.5	S=2.3	S=2.3
Geometrical Correction Factor *(G)*	0.913	0.913	0.912	0.924	0.913	0.87	0.76	0.73
L/W	1.83	1.83	1.82	1.91	1.83	2.27	1	1
W/L	0.54	0.54	0.55	0.52	0.54	0.44	1	1
s/W	0.932	0.932	0.898	0.915	0.932	0.157	0.04	0.115

The absolute sensitivity of the eight cells as a function of the biasing current, between 0-2 mA, is represented in Fig. 4.

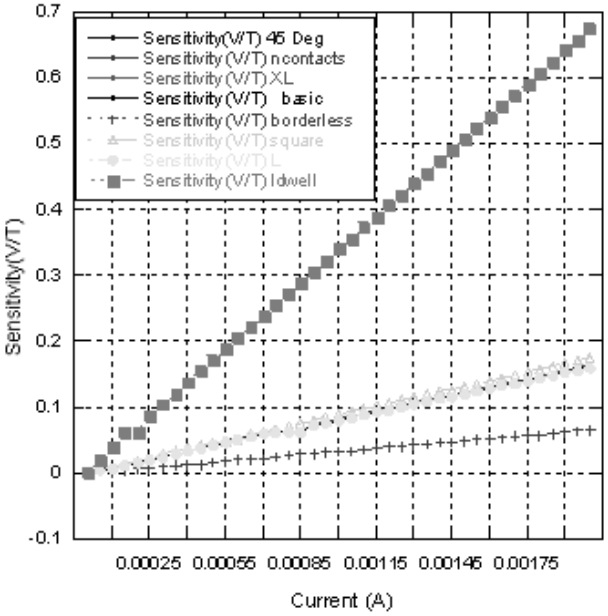

Fig. 4 The measured absolute sensitivity (V/T) of the eight cells as a function of the biasing current (A)

Measurements were made for a perpendicular magnetic field of B=0.497 T and current sweeping between 0-2 mA. The cells behavior with emphasis at 1 mA is summarized in Table 2.

Table 2

Measured vs. computed values for certain parameters of the Hall Cell

Geometry Type	***Basic***	***Low-doped***	***L***	***XL***	***45 Deg***	***Narrow Contacts***	***Borderless***	***Square***
Absolute Sensitivity (V/T) at I_{bias}=1 mA	0.0807	0.3392	0.0804	0.0806	0.0807	0.0822	0.0325	0.0884
Measured V_{Hall} (mV) at I_{bias}=1 mA	40.10	168.58	39.95	40.05	40.10	40.85	16.15	43.93
Computed V_{Hall} (mV) as a function of *G*	39.96	150.29	39.91	40.44	39.96	38.07	33.26	31.95

Power Dissipated (mW) at I_{bias}=1 mA	2.302	5.606	2.202	2.202	2.102	2.503	1.301	4.905
Computed power (mW) as a function of V_{Hall} and G	1.999	7.288	1.949	2.014	1.999	2.437	1.072	1.072

Further on, the graph of the estimated versus measured Hall voltage (mV) is presented, as well as the power dissipated within the device, for I_{bias}=1 mA and a perpendicular magnetic field B=0.497 T.

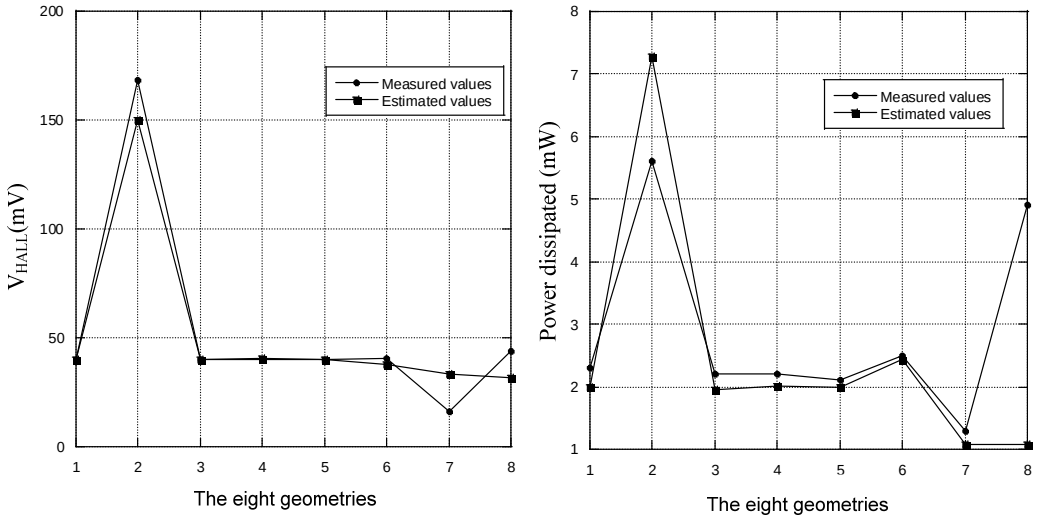

(a) (b)

Fig. 5 Measured vs. estimated values for V_{HALL}(mV) (a) and power dissipated (mW) within the device (b) for I_{bias}=1 mA

For correcting the resistance with the presence of the magnetic field, we used:

$$R = R_0(1 + \mu^2 B^2) \tag{9}$$

After calculations, we obtained an increase of 1.0012 for the resistance in the presence of magnetic field B=0.497 T.

From [1], it is possible to evaluate the highest Hall voltage that can be obtained for different situations that will depend on how the device is monitored. For instance,

imposing the bias current (assuming a long device, i.e. L/W>3), imposing the input voltage (which requires a rather short device, L/W < 0.1), and fixing the power (requiring L/W≈1.3-1.4).

Analysis of the geometrical correction factor behavior

Using MATHEMATICA 7.0, the geometrical factor G is plotted as a function of the length to width ratio L/W and Hall angle, θ_H.

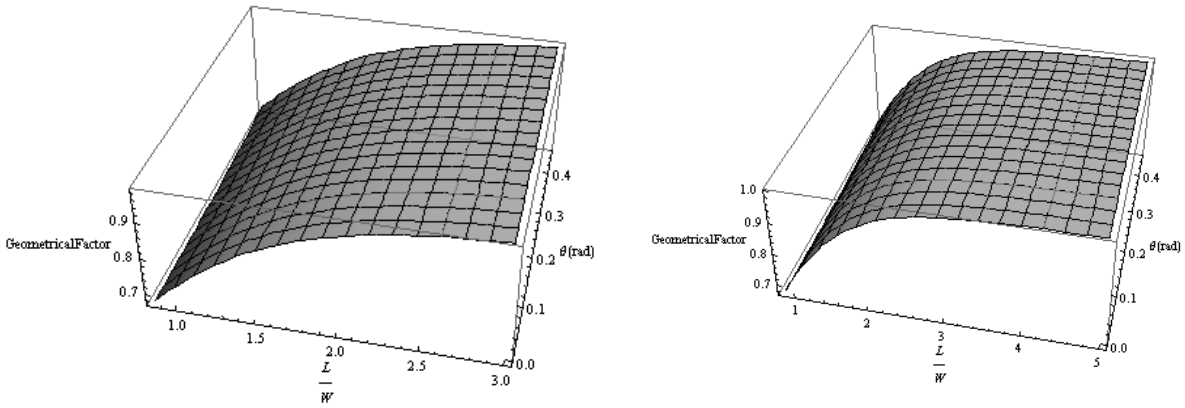

Fig. 6 Representation of the Geometrical correction factor *(G)*, as a function of L/W and Hall angle, θ_H, for 0.85 < L/W < 3 (a) and 0.85 < L/W < 5 (b)

G presented in Eq. (4) will be interpreted in terms of physical meaning, therefore L/W will be evaluated up to 5. In general, for L/W >3, the Hall plate is considerate infinitely long, but we decided to see what happens for 3< L/W<5.

As we can see on Figure 6, for 0.85 < L/W < 3, the geometrical correction factor has a maximum value of 0.98 obtained for L/W=3 and θ_H=0.45 radians. For 0.85 < L/W < 5, the maximum of G is 0.99 and is obviously obtained, due to the behavior of the curve, for the maximum Hall Angle θ_H=0.45 radians and at maximum ratio L/W=5. We observed that for 3< L/W<5, the upper limit of G begins to rapidly increase, from 0.98 to 0.99, but it's only after L/W>5 when G begins to rapidly approach 1.

Indeed, the mathematical limit of G

$$\lim_{L/W\to\infty} G = \lim_{L/W\to\infty}\left(1-\frac{16}{\pi^2}e^{-\frac{\pi L}{2W}}\left(1-\frac{8}{9}e^{-\frac{\pi L}{2W}}\right)\left(1-\frac{\theta_H^2}{3}\right)\right)=1 \tag{10}$$

If we plot the geometrical correction factor as before, but we take L/W to start from 0, we obtain a point of inflexion, with a point of minimum at 0.85 and a decreasing behavior of G with respect to L/W in the range (0, 0.85]. This can be considered as the limit of validity of relation written in Eq. (10).

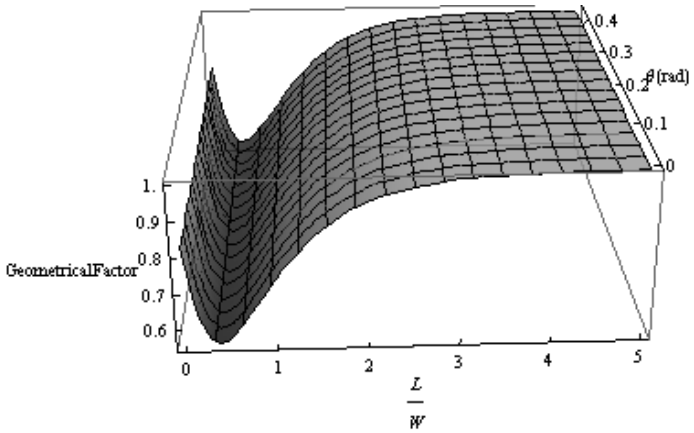

Fig. 7 The presence of the inflexion point close to L/W=0.85

If we include the length of the sensing contacts, we obtain the following simplified expression for the geometrical correction factor

$$G = \left(1 - e^{-\frac{\pi L}{2W}}\right)\left(1 - \frac{2}{\pi}\frac{s}{W}\right) \tag{11}$$

which is valid if L/W >1.5 and is sensing contacts are relatively small, namely s/W < 0.18.

We shall try to find the maximum of the sensitivity, S.

Analytical calculus of the maximum sensitivity as a function of *L*, *W* and of the sensing contacts length, *s*

Using Eq. (6), we write further on

$$dS = S_I I_{bias} dG \tag{12}$$

where dG is the differential of the geometrical factor, written in Eq. (11), more precisely

$$G = G(L,W,s),\ dG = \frac{\partial G}{\partial L}dL + \frac{\partial G}{\partial W}dW + \frac{\partial G}{\partial s}ds \tag{13}$$

The partial derivatives of G with respect to each variable are the following:

$$\frac{\partial G}{\partial L} = \frac{\pi}{2W}\left(1 - \frac{2}{\pi}\frac{s}{W}\right)e^{-\frac{\pi}{2}\frac{L}{W}}$$

$$\frac{\partial G}{\partial W} = \frac{1}{W^2}\left(\frac{Ls}{W} - \frac{2s}{\pi} - \frac{\pi L}{2}\right)e^{-\frac{\pi}{2}\frac{L}{W}} + \frac{2s}{\pi W^2} \tag{15}$$

$$\frac{\partial G}{\partial s} = \left(-\frac{2}{\pi W}\right)\left(1 - e^{-\frac{\pi}{2}\frac{L}{W}}\right) \tag{16}$$

For finding an extremum of a function *f,* we assume a domain A that is open and that *f* is of class C^2 over A. We consider a point *a* of A and we denote the Hessian matrix of *f* at point *a* by $\nabla^2 f(a)$.

If $\nabla f(a) = 0$ and if $\nabla^2 f(a)$ is negatively defined and *f* has a local maximum point at *a*.

Conversely, if $\nabla f(a) = 0$ and $\nabla^2 f(a)$ is positively defined, then *f* has a local minimum point at *a*.

Therefore, in our case, *G* has a point of extremum, *a*, when

$$\begin{cases} \dfrac{\partial G}{\partial W}(a) = 0 \\ \dfrac{\partial G}{\partial L}(a) = 0 \\ \dfrac{\partial G}{\partial s}(a) = 0 \end{cases} \tag{17}$$

To decide whether the extremum point is a maximum or a minimum the second order derivatives should be investigated. The sign of the following determinant must therefore be evaluated.

$$\det\left(\nabla^2 G(a)\right) = \begin{vmatrix} \dfrac{\partial^2 G}{\partial L^2}(a) & \dfrac{\partial^2 G}{\partial L \partial W}(a) & \dfrac{\partial^2 G}{\partial L \partial s}(a) \\ \dfrac{\partial^2 G}{\partial W \partial L}(a) & \dfrac{\partial^2 G}{\partial W^2}(a) & \dfrac{\partial^2 G}{\partial W \partial s}(a) \\ \dfrac{\partial^2 G}{\partial s \partial L}(a) & \dfrac{\partial^2 G}{\partial s \partial W}(a) & \dfrac{\partial^2 G}{\partial s^2}(a) \end{vmatrix} \tag{18}$$

Solving by hand the above system for finding the extrema, we find out that *G* has no maximum. Therefore, it seems that there is no way to maximize *G* unless the ratio *L/W* goes to infinity. MATHEMATICA 7.0 was used to find the maximum value (in this case the upper limits) for *G* for the certain physical intervals investigated, with the best accepted error by the software.

Numerical values obtained with MATHEMATICA 7.0, for the maximum absolute sensitivity

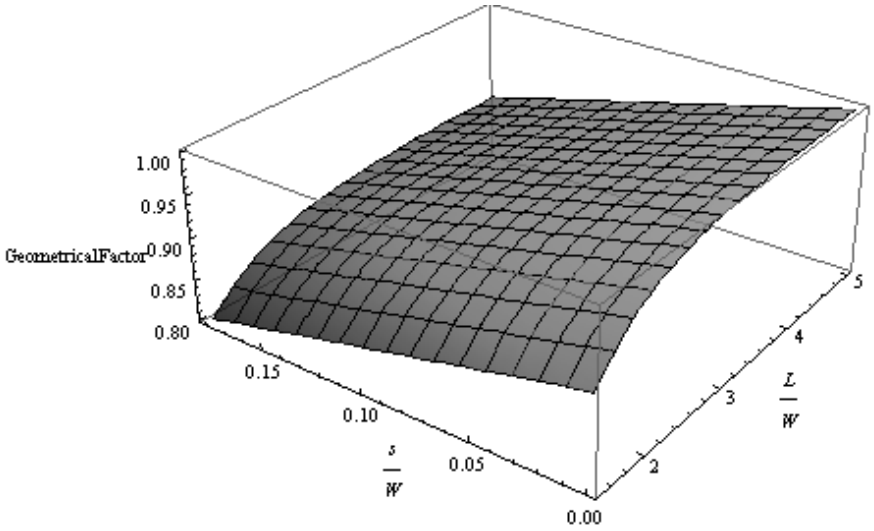

Fig. 8 Variation of the geometrical correction factor G as a function of *L/W* and *s/W*

Using MATHEMATICA 7.0, we find that optimized values for *L/W* and *s/W*, over the interval analyzed giving a geometrical factor close to 1 are.

$$\frac{L}{W} = 5 \;\; and \;\; \frac{s}{W} = 0 \tag{19}$$

This is consistent with the fact that the maximum geometrical correction factor *G*=1 is obtained for infinitely long Hall devices with point-like sensing contacts.

$$\frac{L}{W} \to \infty \;\; and \;\; \frac{s}{W} \to 0 \tag{20}$$

In terms of the eight Hall cells analyzed, seven of them have a carrier concentration n_1, but the lightly-doped cell has a carrier concentration n_2 four times lower than n_1. Since the carrier concentration n_2 is four times lower than n_1, we obtain an absolute sensitivity four times higher.

Assuming that the biasing current is the same, we can calculate the maximum sensitivity. Then, using *G*=1 and the technological parameters we obtain the following theoretical maximum absolute sensitivities for the different doping concentrations with I_{bias}=1 mA.

$$\begin{aligned} S_{\max,n1} &= 0.088 \; V/T \;\; for \;\; n_1 \\ S_{\max,n2} &= 0.33 \; V/T \;\; for \;\; n_2 \end{aligned} \tag{21}$$

The proposed global optimization methodology could be used to find optimum in Hall devices where additional parasitic effects could also impact the sensitivity (doping homogeneity, strain…). The maximization procedure for the geometrical factor and absolute sensitivity could be applied for finding extrema points of functions with constraints. For example, if we have a certain available surface of Si at our disposal,

fixing therefore the value of $A=LW$, and having a s_{min} imposed by the technology for the sensing contacts, we could be thinking about finding W or L giving us a maximum sensitivity (by maximizing G) in this context. In this way, we end up with one variable. This procedure that could guide the designer into tailoring the Hall cell dimensions.

Therefore, Eq. (11) can be rewritten as

$$G = \left(1 - e^{-\frac{\pi A}{2W^2}}\right)\left(1 - \frac{2}{\pi}\frac{s}{W}\right) \tag{22}$$

Keeping constant the contact size provided by the technology (in our case s_{min} =0.35 μm) and having at our disposal a certain area of Si, meaning fixed A, we proceed at maximizing G, now a function of only one variable W, imposing these constraints. Further on, in Figure 9, the variation of L/W with respect to the area A, for different contact sizes, s, which assures a maximum correction factor G, is plotted.

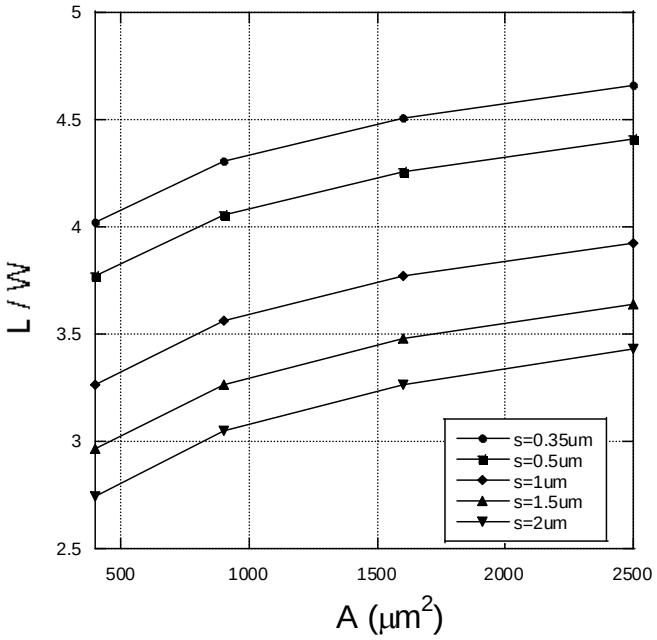

Fig. 9 Variation of L/W with respect to the area A, for different contact sizes s, assuring the maximum correction factor G

Some of the 0.35 μm CMOS Si technology parameters in which the cells were integrated, are summarized in the table below. The N-well doping concentration is usually a Gaussian, but the values of n_1 and n_2 are taken close to the center of the Gaussian. The value of n_2 corresponds to a lightly doped N-well.

Table 3

Technology parameters of interest

Parameter name	Symbol	Units	Value
Mobility	μ	$m^2V^{-1}s^{-1}$	0.0715
Carriers Concentration for N-well	n_1	m^{-3}	8.16e22
	n_2	m^{-3}	2.17e22
Thickness of N-well	t	m	1e-6

5. Conclusions

A series of eight different shapes was integrated in 0.35 μm CMOS Si technology. A device level analysis of the Hall cell geometries, in terms of sensitivity, V_{HALL}, power dissipated, etc. was performed. Each structure was geometrically characterized by the L/W, s/W ratio and geometrical correction factor, G. The impact of the geometrical parameters and how these affect the device performances was studied.

With the proposed technology, a maximum absolute sensitivity $S_{max,n1}$=0.088 V/T was obtained with the carrier concentration n_1 and $S_{max,n2}$=0.33 V/T for lightly doped N-wells, with a carrier concentration n_2. As the absolute sensitivity is proportional to G, cells with G close to unity will assure obtaining the maximum absolute sensitivity.

MATHEMATICA 7.0 was used for evaluating the maximum values of the geometrical correction factor, for the two expressions, both in terms of L/W, θ_H and L/W and s/W respectively, for the intervals imposed by the physical interpretation of Hall devices.

For $0.85 < L/W < 3$, the geometrical correction factor has a maximum value of 0.98 obtained for L/W=3 and θ_H=0.45 radians. For $0.85 < L/W < 5$, G approaches 0.99. For values of $L/W > 5$, the geometrical factor begins to asymptotically tend to 1. The geometrical correction factor G begins to asymptotically tend to 1, for infinitely long devices ($L/W > 5$) with point-like sensing contacts ($s \rightarrow 0$).

Measurements versus simulations were investigated, for all eight cells, in terms of V_{HALL} and power dissipated. Because the cells were measured with an automated system, the same biasing conditions were applied to all the 8 cells. A biasing current between 0-2 mA, together with a compliance voltage for the current source of 5 V, was sufficient for testing the majority of cells, but for the low doped and square, saturation begins to appear for higher biasing currents. However, for the absolute sensitivity curves for these two cells, an extrapolation was done between 1 and 2 mA of biasing current. Due to the high values of the resistances for the low-doped cells (approximately 5 kΩ) the values for the measured versus estimated power dissipated

show some discrepancies, due to the effective saturation that might appear when biasing the cells with higher currents.

V_{HALL} has an average value of 40 mV for I_{bias}=1 mA and B=0.497 T, with a value four times higher for lightly doped N-wells. For the tested geometries, the highest Hall voltage was obtained with a given bias current, if a Hall device was long, let's say with $L/W \approx 2$.

The proposed maximization procedure for the geometrical correction factor and subsequent sensitivity maximization was used for guiding the designer in finding the optimum dimensions (*W, L*) for the Hall cell, subject to some technological constraints (imposed sensing contact size) and Si surface availability.

Ackowledgements

This work has been supported by Swiss Innovation Promotion Agency CTI (Project 9591.1) and the company LEM - Geneva, Switzerland.

R E F E R E N C E S

[1] *R.S Popovic*, Hall Effect Devices, Second Edition, Institute of Physics Publishing, 2004

[2] *T. Kramer, V. Krueckl, E.J. Heller, R.E. Parrott*, Self-consistent calculation of electric potentials in Hall devices, Physical Review B, Vol. **81**, 205306, 2010

[3] Honeywell References, Micro Switch Sensing and Control, Chapter 2, Hall Effect Sensors

[4] *S.V. Lozanova, C.S. Roumenin*, Parallel-Field Silicon Hall Effect Microsensors with Minimal Design Complexity, IEEE Sensors Journal, Vol. **9**, No. 7, 761, 2009

[5] *R.S. Popovic, Z. Randjelovic, D. Manic*, Integrated Hall-effect magnetic sensors, Sensors and Actuators A, Vol. **91**, 2001, pp.46-50

[6] *M. Kayal, M. Pastre*, Automatic calibration of Hall sensor microsystems, Microelectronics Journal Vol. **37**, 2006, pp. 1569–1575

[7] *J. Pascal, L. Hébrard, J.-B. Kammerer V. Frick, J.-P. Blondé*, First vertical Hall Device in standard 0.35 μm CMOS technology, Sensors and Actuators A: Physical, Vol. **147**, 2008, pp. 41-46